

Aspartate 112 is the selectivity filter of the human voltage-gated proton channel

Boris Musset^{1*}, Susan M. E. Smith^{2*}, Sindhu Rajan³, Deri Morgan¹, Vladimir V. Cherny¹ & Thomas E. DeCoursey¹

The ion selectivity of pumps and channels is central to their ability to perform a multitude of functions. Here we investigate the mechanism of the extraordinary selectivity of the human voltage-gated proton channel¹, H_V1 (also known as HVCN1). This selectivity is essential to its ability to regulate reactive oxygen species production by leukocytes^{2–4}, histamine secretion by basophils⁵, sperm capacitation⁶, and airway pH⁷. The most selective ion channel known, H_V1 shows no detectable permeability to other ions¹. Opposing classes of selectivity mechanisms postulate that (1) a titratable amino acid residue in the permeation pathway imparts proton selectivity^{1,8–11}, or (2) water molecules ‘frozen’ in a narrow pore conduct protons while excluding other ions¹². Here we identify aspartate 112 as a crucial component of the selectivity filter of H_V1. When a neutral amino acid replaced Asp 112, the mutant channel lost proton specificity and became anion-selective or did not conduct. Only the glutamate mutant remained proton-specific. Mutation of the nearby Asp 185 did not impair proton selectivity, indicating that Asp 112 has a unique role. Although histidine shuttles protons in other proteins, when histidine or lysine replaced Asp 112, the mutant channel was still anion-permeable. Evidently, the proton specificity of H_V1 requires an acidic group at the selectivity filter.

Voltage-gated proton channels are considered specific (perfectly selective) for protons, because no evidence exists for permeation of anything but H⁺. Specificity, combined with a large deuterium isotope effect⁹ and extraordinarily strong temperature dependence of conduction¹⁰ suggests a permeation pathway more complex than a simple water wire, as exists in gramicidin¹³. All proton conduction seems consistent with a hydrogen-bonded chain (HBC) mechanism¹⁴; a HBC including a titratable group could explain several unique properties of H_V1 (ref. 1), especially proton selectivity¹⁴. Yet in a recent study, mutation of each titratable amino acid in all four transmembrane helices of H_V1 failed to abolish conduction¹². Thus, the mechanism producing proton selectivity remained unknown.

We noticed that a human gene, *C15orf27* (of unknown function), contains a predicted voltage sensor domain (VSD) that shares 25% sequence identity and 52% similarity (<http://www.ebi.ac.uk/Tools/emboss/align/needle>) with the VSD of H_V1, and includes three Arg residues in the S4 transmembrane helix that are conserved among all known H_V1 homologues. Phylogenetic analysis of VSD sequences (Supplementary Fig. 1) reveals that a group comprising H_V1, *C15orf27* and voltage-sensitive phosphatase (VSP) sequences separated early from the two phylogenetically distinct groups of depolarization activated VSDs described previously (K_V channels and Na_V/Ca_V channels), supporting the modular evolution of VSD-containing proteins¹⁵. Furthermore, H_V1 VSDs occupy a discrete lineage, distinct from those of VSP and *C15orf27* orthologues.

When we cloned the *C15orf27* gene and expressed the product in HEK-293 or COS-7 cells, the green fluorescent protein (GFP)-tagged protein localized at the plasma membrane (Supplementary Fig. 2), but we detected no currents beyond those in non-transfected cells. We

reasoned that substitutions based on sequence elements that differ between H_V1 and *C15orf27* should be structurally tolerated while revealing residues responsible for proton conduction. We therefore mutated residues that are perfectly conserved in 21 H_V1 family members and differ between *C15orf27* and H_V1. We replaced five candidate residues in H_V1 (D112, D185, N214, G215 and S219) (Fig. 1a, b) with the corresponding residue in *C15orf27*. Four mutants exhibited large currents under whole-cell voltage clamp (Fig. 1d). The reversal (zero current) potential, V_{rev} , measured at several pH_o and pH_i (external and internal pH, respectively), was close to the Nernst potential for protons, E_{H} (Fig. 1c), demonstrating proton selectivity. D112V mutants localized to the plasma membrane (Supplementary Fig. 3), but showed no convincing current (Fig. 1d). Some D112V-transfected HEK-293 or COS-7 cells (and non-transfected cells) had small native proton currents. H140A/H193A double mutants^{16,17}, in which the two Zn²⁺-binding His residues are neutralized, resemble wild type, with similar Δ pH-dependent gating¹², and V_{rev} near E_{H} (Supplementary Fig. 4). We expressed mutants in this Zn²⁺-insensitive background (D112X/A/A) to distinguish their currents from native currents that are abolished by 100 μ M Zn²⁺ at pH_o 7.0. We tentatively concluded that Asp 112 is crucial to proton conduction.

The absence of detectable currents in D112V led us to make other D112X substitutions. These mutants (Fig. 2a) showed slowly activating outward currents upon depolarization that resembled H_V1 currents. As reported previously¹², Asp 112 mutation had little effect on the Δ pH dependence of gating. The proton conductance–voltage ($g_{\text{H}}-V$) relationship of all D112X mutants shifted roughly –60 mV when pH_o increased from 5.5 to 7.0 (Supplementary Fig. 5), as in wild-type channels^{1,8,18}. Mutation of Asp 112 did influence channel opening and closing kinetics (Supplementary Table 2).

Measurements of V_{rev} in Asp 112 mutants showed a marked departure from wild-type H_V1 properties. At symmetrical pH 5.5, V_{rev} was near 0 mV (not shown). At pH_o 7.0, pH_i 5.5 (Fig. 2a, column 3), wild-type channels reversed near E_{H} (–87 mV), indicating proton selectivity. But for all mutants except D112E, V_{rev} was substantially positive to E_{H} (Fig. 2b), ranging from –58 mV (D112H) to –13 mV (D112N). Substitutions at Asp 112 eliminated the proton specificity that distinguishes H_V1 from all other ion channels¹. A previous study described currents in D112A and D112N mutants¹², but did not report V_{rev} .

We expected that loss of proton selectivity would result in nonselective permeation of cations. Surprisingly, V_{rev} did not change detectably when Na⁺, K⁺, *N*-methyl-D-glucamine⁺ or TEA⁺ (tetraethylammonium⁺) replaced TMA⁺ (tetramethylammonium⁺) (Supplementary Table 4). To test anion against cation selectivity, we adopted the classical tactic of replacing a fraction of the bath solution with isotonic sucrose¹⁹. The Nernst equation predicts that dilution of all extracellular ions except H⁺ and OH[–] (leaving internal ion concentrations unchanged) will shift V_{rev} negatively for a cation-selective channel, but positively for an anion-selective one. Despite the tenfold reduction of buffer concentration, direct measurement confirmed that pH remained constant.

¹Department of Molecular Biophysics & Physiology, Rush University Medical Center, Chicago, Illinois 60612, USA. ²Department of Pathology, Emory School of Medicine, Atlanta, Georgia 30322, USA.

³Department of Medicine, University of Chicago, Chicago, Illinois 60637, USA.

*These authors contributed equally to this work.

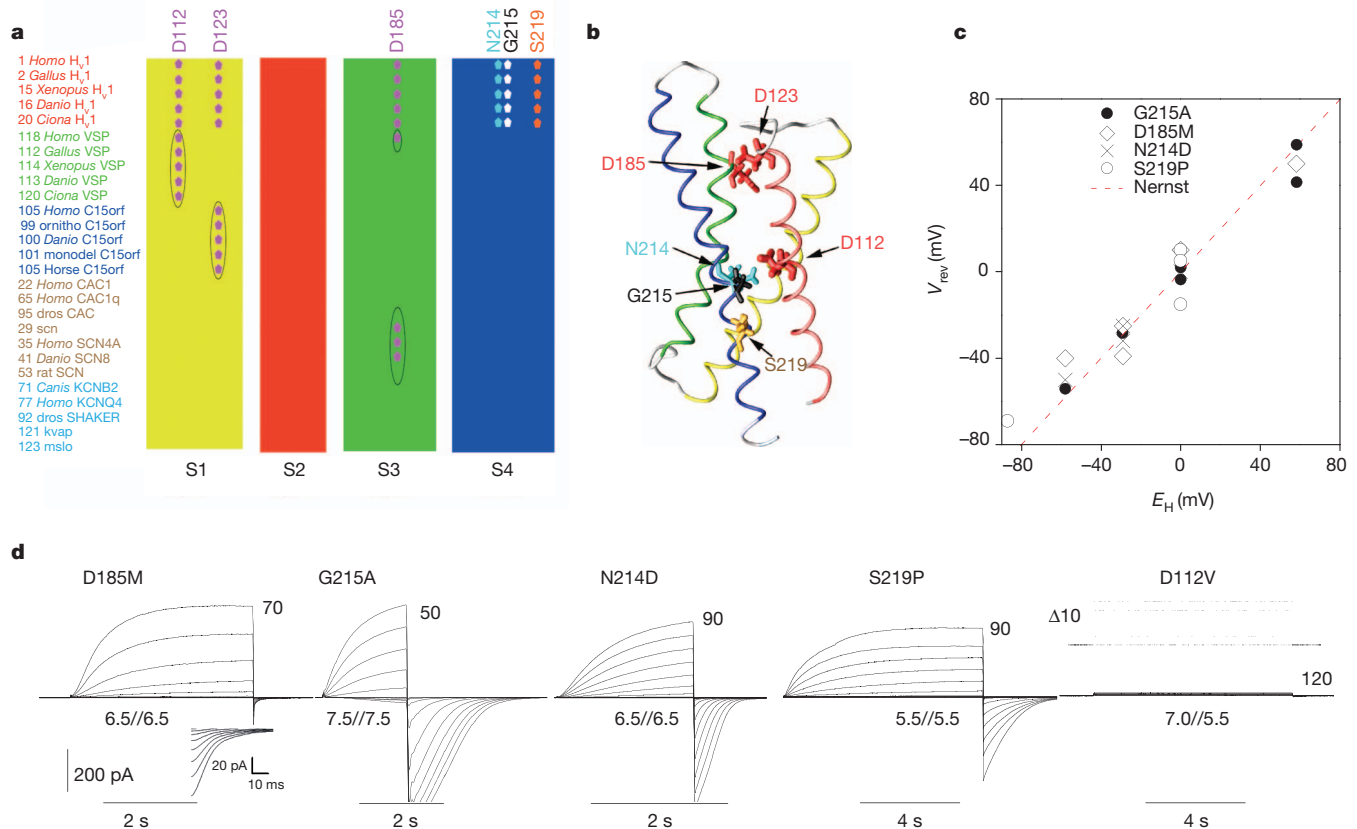


Figure 1 | Identification of five key amino acids that differ in H_V1 and C15orf27, and the currents generated in a heterologous expression system by H_V1 mutants in which H_V1 residues were replaced by the corresponding amino acid in the non-conducting C15orf27. **a**, Representative subset of multiple sequence alignment of 122 VSDs, only transmembrane helices are shown. Gene families include H_V1, voltage-sensitive phosphatases, C15orf27, Ca²⁺ and Na⁺ channels, and K⁺ channels (see Supplementary Fig. 1). **b**, Location of the key amino acids in the open H_V1 channel VSD viewed from the side (membrane), based on a homology model¹⁷. **c**, V_{rev} in the four

conducting mutants is near E_{H} (dashed line), indicating proton selectivity. V_{rev} was measured using tail currents; in G215A V_{rev} was positive to threshold and was observed directly. **d**, Voltage-clamp current families in cells expressing H_V1 mutants. Depolarizing pulses were applied in 10-mV increments from a holding voltage, $V_{\text{hold}} = -40$ mV (D185M, D112V), -60 mV (G215A, S219P), or -90 mV (N214D), with the most positive pulse labelled. After membrane repolarization, an inward 'tail current' is seen as channels close (see inset for D185M); pH is given as pH_o/pH_i . D112V showed no clear current.

Figure 3 illustrates determination of V_{rev} from tail currents in a D112H-transfected cell at pH 5.5/5.5 (pH_o/pH_i) in methanesulphonate⁻ (CH_3SO_3^- ; Fig. 3a) or Cl^- solution (Fig. 3c), and after 90% reduction of external ionic strength (Figs 3b, d). Surprisingly, for all Asp 112 mutants, sucrose shifted V_{rev} positively (Supplementary Fig. 6), indicating anion selectivity both in CH_3SO_3^- (Fig. 3e) and Cl^- solutions (Fig. 3f). For H_V1 and D112E, V_{rev} did not change, reaffirming their proton specificity. Neutralization of a single Asp residue converts a proton channel into a predominantly anion selective channel. Thus, Asp 112 mediates charge selectivity as well as proton selectivity.

To confirm anion permeability of Asp 112 mutants, we replaced the main external anion, CH_3SO_3^- , with Cl^- . Consistent with previous studies¹, V_{rev} in H_V1 was unchanged. As shown in D112H (Fig. 3a, c), V_{rev} shifted negatively in Cl^- solutions in all mutants (except D112E), indicating that Cl^- is more permeant than the larger CH_3SO_3^- anion (Fig. 3g). That all conducting non-acidic mutants showed Cl^- permeability indicates that Asp 112 mediates not only proton selectivity, but also charge selectivity. Currents were smaller than wild type in cells expressing some mutants (Supplementary Fig. 7), suggesting a smaller unitary conductance. Evidently, these channels conduct anions, but not very well.

Although the mutant channels have diminished selectivity, V_{rev} did shift negatively when pH_o increased from 5.5 to 7.0 (Fig. 2b). Because

these solutions differ mainly in buffer species and concentrations of H^+ and OH^- , Asp 112 mutants must have significant permeability to H^+ and/or OH^- . The Goldman-Hodgkin-Katz equation shows how V_{rev} depends on ion concentrations:

$$V_{\text{rev}} = \frac{RT}{zF} \log \frac{P_{\text{Cl}^-} [\text{Cl}^-]_i + P_{\text{CH}_3\text{SO}_3^-} [\text{CH}_3\text{SO}_3^-]_i + P_{\text{OH}^-} [\text{OH}^-]_i + P_{\text{H}^+} [\text{H}^+]_o}{P_{\text{Cl}^-} [\text{Cl}^-]_o + P_{\text{CH}_3\text{SO}_3^-} [\text{CH}_3\text{SO}_3^-]_o + P_{\text{OH}^-} [\text{OH}^-]_o + P_{\text{H}^+} [\text{H}^+]_i}$$

where R is the gas constant, T the absolute temperature (Kelvin), z the ionic valence ($= 1$), F is Faraday's constant and P is permeability.

Ions with greater permeability dominate V_{rev} . Permeation of H^+ and OH^- are difficult to distinguish because they have the same Nernst potential¹. The data can be interpreted assuming permeation of either (Supplementary Table 3), but the anion selectivity of Asp 112 mutants and the pH dependence of sucrose effects (Figs 3e, f) support OH^- permeation. The relative permeability of conducting Asp 112 mutants was OH^- (or H^+) $>$ $\text{Cl}^- >$ CH_3SO_3^- .

Although Asp 112 is essential to selectivity, other acidic groups might participate. We mutated Asp 185, located in the presumed conduction pore (Fig. 1b)^{12,17}. However, like D185M (Fig. 1b), D185V, D185A and D185N remained proton-selective (Supplementary Fig. 8). As evidence against additive effects, the double mutant D112N/D185M did not differ from D112N (Supplementary Fig. 8).

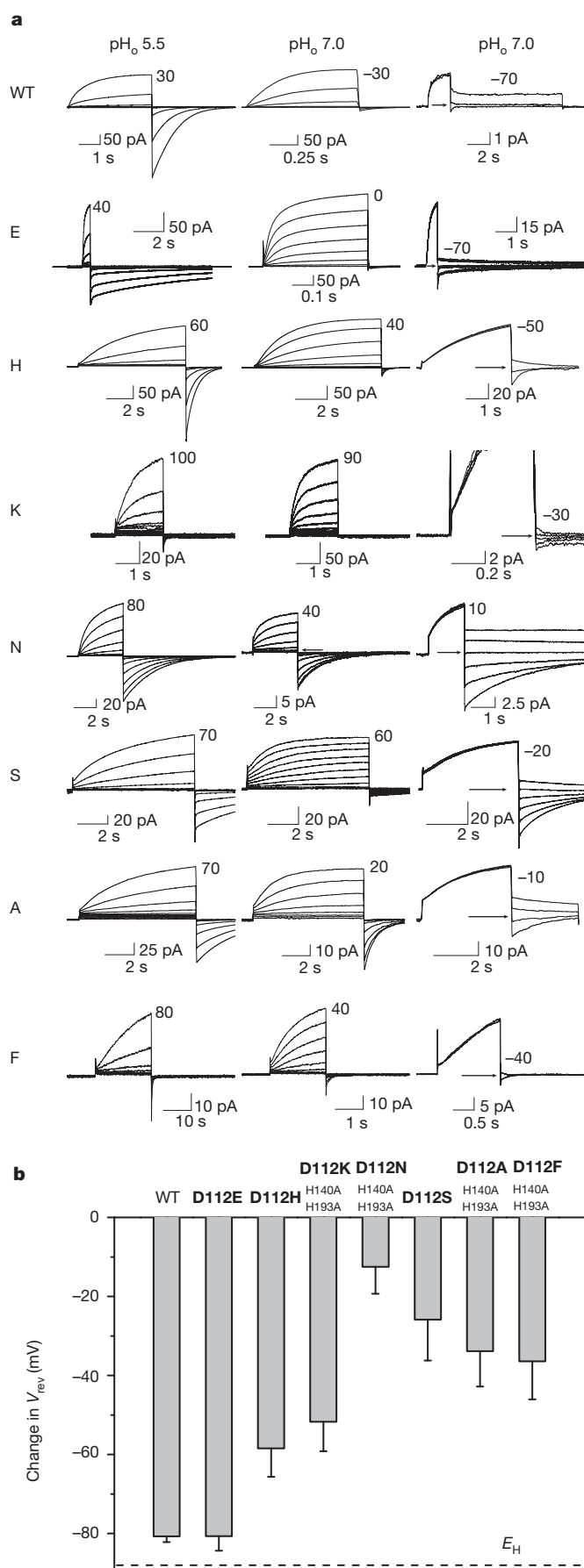


Figure 2 | Currents in Asp 112 mutants resemble proton currents, but are not. **a**, Currents generated by wild type (WT), D112E, D112H, D112K/A/A, D112N/A/A, D112S, D112A/A/A and D112F/A/A in COS-7 cells (pH_i 5.5) at pH_o 5.5 (column 1) or 7.0 (column 2), during families of pulses in 10 mV increments up to indicated voltages. Tail currents at pH_o 7.0 (column 3) reveal that V_{rev} deviates from E_{H^+} , indicating loss of proton selectivity. At pH_o 5.5 V_{hold} was -40 mV (-60 mV for WT). At pH_o 7.0 V_{hold} was -40 mV (K, N, S), -50 mV (F), -60 mV (H, A), -80 mV (E), or -90 mV (WT); V_{pre} was -65 mV (WT), -40 mV (E), -10 mV (H), $+50$ mV (K), $+40$ mV (N, S), or $+20$ mV (A, F). V_{rev} (arrows) was determined from the amplitude and direction of tail current decay. For D112N, V_{rev} was above $V_{threshold}$ and was evident during pulse families. **b**, Shift in V_{rev} when the TMACH₃SO₃ bath solution was changed from pH 5.5 to 7.0. There is no difference between WT and D112E, but the shift in all other mutants is smaller than WT ($P < 0.001$, by one-way ANOVA followed by Tukey's test, $n = 7, 4, 9, 8, 6, 7, 9$ and 4). Error bars in **b** are s.e. Dashed line shows E_{H^+} .

Consistent with earlier predictions that a titratable amino acid provides the selectivity filter of H_v1 (refs 1, 8–11), only channels with acidic residues (Glu or Asp) at position 112 manifested proton specificity. Asp 112 lies at the constriction of the presumed pore (Fig. 1b), a logical location for a selectivity filter, and just external to the postulated gating charge transfer centre²⁰. Our original prediction envisioned selectivity arising from protonation/deprotonation of a residue during conduction, but other mechanisms are possible. For example, proton selectivity of the influenza A M₂ viral proton channel has been explained by (1) immobilized water²¹, (2) successive proton transfer and release by His 37 (refs 22, 23) and (3) delocalization of the proton among His 37 and nearby water molecules²⁴.

The Cl⁻ permeability of D112H was completely unexpected, given strong precedents for His imparting proton selectivity to channels. Histidine shuttles protons in K⁺ or Na⁺ channel VSDs with Arg→His mutations^{25–27}, in carbonic anhydrase²⁸ and in M₂ channels^{22,23}. However, these molecules are not proton-specific^{27,29}. Evidently, His shuttles protons, but does not guarantee proton selectivity. In H_v1, Asp 112 (or Glu 112 in D112E) excludes anions, resulting in proton-specific conduction. When protonated, Glu and Asp are neutral whereas His is cationic, which may explain why D112H fails to exclude anions.

The anion selectivity of neutral Asp 112 mutants indicates that electrostatic forces due to the charge distribution in the rest of the channel deter cation permeation, and that the cation selectivity of the wild-type channel is due to the anionic charge of Asp 112. Asp 185 does not participate directly in selectivity (Supplementary Fig. 8). VSP family members possess the equivalent of Asp 112 (Fig. 1a), yet conduct no current³⁰, illustrating that Asp 112 requires a specific microenvironment to achieve selectivity. Although permeation of Cl⁻ and CH₃SO₃⁻ suggests a wide pore in D112X mutants, local geometry might differ in wild-type channels due to the presence of anionic Asp 112.

Regulation of voltage gating by ΔpH is distinct from permeation. Pathognomonic of H_v1 is a strict correlation between the g_H - V relationship and V_{rev} , in which $V_{threshold}$ shifts 40 mV per unit change in ΔpH (ref. 8). The ΔpH dependence persisted in mutants with shifted g_H - V relationships¹². Here we show uncoupling of V_{rev} and voltage gating. Asp 112 mutants retained normal ΔpH dependence (Supplementary Fig. 5), despite the dissociation of V_{rev} from ΔpH (Fig. 2 and Supplementary Fig. 9). This uncoupling of pH control of gating from permeation speaks against any mechanism that invokes regulation by local proton concentration in the vicinity of S4 Arg residues¹².

In summary, Asp 112 is a critical component of the selectivity filter of H_v1, crucial to both proton selectivity and charge selectivity. That D112E was proton-selective, but D112H conducted anions indicates that this proton channel requires an acid at the selectivity filter. That neutralization of nearby Asp 185 did not affect selectivity suggests that Asp 112 has a unique role.

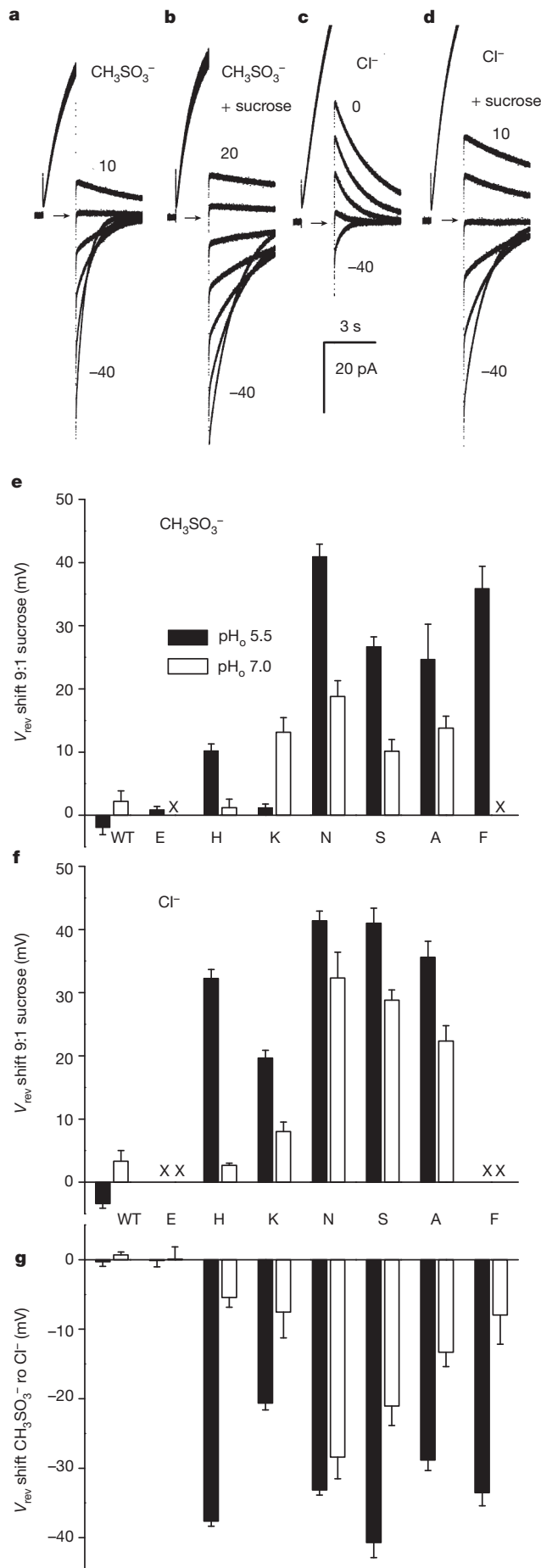


Figure 3 | Dilution of ionic strength by 90% with isotonic sucrose shifted V_{rev} positively, indicating that most Asp112 mutants are anion-selective. **a**, Measurement of V_{rev} by tail currents in a cell transfected with D112H at pH 5.5/5.5, and **b**, after sucrose. **c**, V_{rev} in the same cell in pH 5.5 Cl^- solution, and **d**, after sucrose. Arrows indicate zero current. $V_{hold} = -40$ mV, $V_{pre} = +60$ mV. **e**, Mean shifts of V_{rev} with decreasing ionic strength in $CH_3SO_3^-$ solutions or **f**, in Cl^- solutions. Each value was determined in 3–6 cells. X = not done. **g**, Shifts of V_{rev} when $CH_3SO_3^-$ was replaced by Cl^- . Values for WT and D112E do not differ significantly from 0 mV. For all anion-selective mutants except D112N, the difference between shifts at pH 5.5 and 7.0 was significant ($P < 0.001$, one-way ANOVA followed by Tukey's test; $n = 3-8$). Error bars in **e-g** are s.e.

METHODS SUMMARY

The pipette solution (also used externally) contained (in mM) 130 $TMACH_3SO_3$, 2 $MgCl_2$, 2 EGTA, 80 MES (2-(*N*-morpholino)ethanesulphonic acid), titrated to pH 5.5 with ~ 20 TMAOH. In the pH 5.5 TMAOH solution, TMAOH replaced $TMACH_3SO_3$. Bath solutions at pH 7.0 had (mM) 90 $TMACH_3SO_3$ or TMAOH, 3 $CaCl_2$, 1 EGTA, 100 BES and 36–40 TMAOH. For experiments with Zn^{2+} , solutions contained PIPES without EGTA. Experiments were done at 20–25 °C. Currents are shown without leak correction. V_{rev} data were corrected for liquid junction potentials measured in each solution¹⁹.

Full Methods and any associated references are available in the online version of the paper at www.nature.com/nature.

Received 5 April; accepted 13 September 2011.

Published online 23 October 2011.

- DeCoursey, T. E. Voltage-gated proton channels and other proton transfer pathways. *Physiol. Rev.* **83**, 475–579 (2003).
- Capasso, M. *et al.* HVCN1 modulates BCR signal strength via regulation of BCR-dependent generation of reactive oxygen species. *Nature Immunol.* **11**, 265–272 (2010).
- DeCoursey, T. E., Morgan, D. & Cherny, V. V. The voltage dependence of NADPH oxidase reveals why phagocytes need proton channels. *Nature* **422**, 531–534 (2003).
- Henderson, L. M., Chappell, J. B. & Jones, O. T. G. The superoxide-generating NADPH oxidase of human neutrophils is electrogenic and associated with an H^+ channel. *Biochem. J.* **246**, 325–329 (1987).
- Musset, B. *et al.* A pH-stabilizing role of voltage-gated proton channels in IgE-mediated activation of human basophils. *Proc. Natl Acad. Sci. USA* **105**, 11020–11025 (2008).
- Lishko, P. V., Botchkina, I. L., Fedorenko, A. & Kirichok, Y. Acid extrusion from human spermatozoa is mediated by flagellar voltage-gated proton channel. *Cell* **140**, 327–337 (2010).
- Iovannisci, D., Illek, B. & Fischer, H. Function of the HVCN1 proton channel in airway epithelia and a naturally occurring mutation, M91T. *J. Gen. Physiol.* **136**, 35–46 (2010).
- Cherny, V. V., Markin, V. S. & DeCoursey, T. E. The voltage-activated hydrogen ion conductance in rat alveolar epithelial cells is determined by the pH gradient. *J. Gen. Physiol.* **105**, 861–896 (1995).
- DeCoursey, T. E. & Cherny, V. V. Deuterium isotope effects on permeation and gating of proton channels in rat alveolar epithelium. *J. Gen. Physiol.* **109**, 415–434 (1997).
- DeCoursey, T. E. & Cherny, V. V. Temperature dependence of voltage-gated H^+ currents in human neutrophils, rat alveolar epithelial cells, and mammalian phagocytes. *J. Gen. Physiol.* **112**, 503–522 (1998).
- DeCoursey, T. E. & Cherny, V. V. Voltage-activated hydrogen ion currents. *J. Membr. Biol.* **141**, 203–223 (1994).
- Ramsey, I. S. *et al.* An aqueous H^+ permeation pathway in the voltage-gated proton channel Hv1. *Nature Struct. Mol. Biol.* **17**, 869–875 (2010).
- Levitt, D. G., Elias, S. R. & Hautman, J. M. Number of water molecules coupled to the transport of sodium, potassium and hydrogen ions via gramicidin, nonactin or valinomycin. *Biochim. Biophys. Acta* **512**, 436–451 (1978).
- Nagle, J. F. & Morowitz, H. J. Molecular mechanisms for proton transport in membranes. *Proc. Natl Acad. Sci. USA* **75**, 298–302 (1978).
- Nelson, R. D., Kuan, G., Saier, M. H. Jr & Montal, M. Modular assembly of voltage-gated channel proteins: a sequence analysis and phylogenetic study. *J. Mol. Microbiol. Biotechnol.* **1**, 281–287 (1999).
- Ramsey, I. S., Moran, M. M., Chong, J. A. & Clapham, D. E. A voltage-gated proton-selective channel lacking the pore domain. *Nature* **440**, 1213–1216 (2006).
- Musset, B. *et al.* Zinc inhibition of monomeric and dimeric proton channels suggests cooperative gating. *J. Physiol. (Lond.)* **588**, 1435–1449 (2010).
- Musset, B. *et al.* Detailed comparison of expressed and native voltage-gated proton channel currents. *J. Physiol. (Lond.)* **586**, 2477–2486 (2008).
- Barry, P. H. The reliability of relative anion-cation permeabilities deduced from reversal (dilution) potential measurements in ion channel studies. *Cell Biochem. Biophys.* **46**, 143–154 (2006).
- Tao, X., Lee, A., Limapichat, W., Dougherty, D. A. & MacKinnon, R. A gating charge transfer center in voltage sensors. *Science* **328**, 67–73 (2010).

21. Sansom, M. S. P., Kerr, I. D., Smith, G. R. & Son, H. S. The influenza A virus M2 channel: a molecular modeling and simulation study. *Virology* **233**, 163–173 (1997).
22. Hu, F., Luo, W. & Hong, M. Mechanisms of proton conduction and gating in influenza M2 proton channels from solid-state NMR. *Science* **330**, 505–508 (2010).
23. Venkataraman, P., Lamb, R. A. & Pinto, L. H. Chemical rescue of histidine selectivity filter mutants of the M2 ion channel of influenza A virus. *J. Biol. Chem.* **280**, 21463–21472 (2005).
24. Acharya, R. *et al.* Structure and mechanism of proton transport through the transmembrane tetrameric M2 protein bundle of the influenza A virus. *Proc. Natl Acad. Sci. USA* **107**, 15075–15080 (2010).
25. Starace, D. M. & Bezanilla, F. Histidine scanning mutagenesis of basic residues of the S4 segment of the *Shaker* K⁺ channel. *J. Gen. Physiol.* **117**, 469–490 (2001).
26. Starace, D. M. & Bezanilla, F. A proton pore in a potassium channel voltage sensor reveals a focused electric field. *Nature* **427**, 548–553 (2004).
27. Sokolov, S., Scheuer, T. & Catterall, W. A. Ion permeation and block of the gating pore in the voltage sensor of Nav_v1.4 channels with hypokalemic periodic paralysis mutations. *J. Gen. Physiol.* **136**, 225–236 (2010).
28. Tu, C. K., Silverman, D. N., Forsman, C., Jonsson, B. H. & Lindskog, S. Role of histidine 64 in the catalytic mechanism of human carbonic anhydrase II studied with a site-specific mutant. *Biochemistry* **28**, 7913–7918 (1989).
29. Leiding, T., Wang, J., Martinsson, J., DeGrado, W. F. & Årsköld, S. P. Proton and cation transport activity of the M2 proton channel from influenza A virus. *Proc. Natl Acad. Sci. USA* **107**, 15409–15414 (2010).
30. Murata, Y., Iwasaki, H., Sasaki, M., Inaba, K. & Okamura, Y. Phosphoinositide phosphatase activity coupled to an intrinsic voltage sensor. *Nature* **435**, 1239–1243 (2005).

Supplementary Information is linked to the online version of the paper at www.nature.com/nature.

Acknowledgements We thank P. H. Barry, D. Gillespie, V. S. Markin, J. F. Nagle, R. Pomès, D. Silverman and V. Sokolov for discussions or comments on the manuscript. Supported by NSF grant MCB-0943362 (S.M.E.S. and T.E.D.) and NIH grant GM087507 (T.E.D.). The content is solely the responsibility of the authors and does not necessarily represent the views of the National Institute of General Medical Sciences or the National Institutes of Health.

Author Contributions S.R. identified the similarity of C15orf27 to H_v1 and cloned the C15orf27 gene; S.M.E.S. conceived the strategic approach based on molecular model, sequence and phylogenetic analysis; S.R. and S.M.E.S. created mutants; T.E.D., B.M. and V.V.C. designed experiments; B.M., D.M. and V.V.C. recorded, analysed and interpreted data; T.E.D. wrote the manuscript; all authors read and approved the manuscript.

Author Information Reprints and permissions information is available at www.nature.com/reprints. The authors declare no competing financial interests. Readers are welcome to comment on the online version of this article at www.nature.com/nature. Correspondence and requests for materials should be addressed to T.E.D. (tdecours@rush.edu).

METHODS

Exhaustive searches to identify H_V1 homologues were performed using protein BLAST and PSI-BLAST. A sample of VSDs from K^+ , Na^+ and Ca^{2+} channels (that open with depolarization like H_V1 , and in addition one that opens with hyperpolarization), along with putative H_V1 , VSP and C15orf27 homologues were chosen. For cation channels, we sampled from the range of subfamilies, from the VSD repeats within Na^+ and Ca^{2+} channels, and from the range of species. VSD sequences, including crystallized K^+ channels (PDB accessions 1ORS, 2R9R and 2A79), were aligned using Promals3D³¹, which incorporates structural information, allowing high-confidence identification of VSD boundaries. Sequences were trimmed to the VSD, realigned with Promals3D, and the resulting alignment was analysed with PhyML (maximum likelihood)³² and Protpars (maximum parsimony)³³ at the Mobyly portal³⁴. Trees were visualized with TreeDyn³⁵ and iTOL³⁶. Parsimony (not shown) and maximum likelihood trees had similar topology, including H_V1 and C15orf27 families separating into discrete branches. A homology model of the VSD of H_V1 was constructed as described previously¹⁷.

The C15orf27 clone was PCR-amplified from human cerebellum and subcloned into pcDNA3.1(+) expression vector (Invitrogen). The coding sequence of human H_V1 (*HVCN1*) was cloned into either pcDNA3.1(-) or pQBI25-fC3 (to make GFP- H_V1) vectors as described previously¹⁶. Site-directed mutants were created using the Stratagene QuikChange (Agilent) procedure according to the manufacturer's instructions. All the positive clones were sequenced to confirm the presence of the introduced mutation. HEK-293 or, more often COS-7 cells were grown to ~80% confluency in 35-mm cultures dishes, usually by seeding cells 1 day ahead of transfection. Cells were transfected with 0.4–0.5 μ g of the appropriate cDNA using Lipofectamine 2000 (Invitrogen). After 6 h at 37 °C in 5% CO_2 ,

the cells were trypsinized and replated onto glass cover slips at low density for patch clamp recording the following day. We selected green cells under fluorescence for recording. Patch-clamp methods were described previously¹⁸.

The main pipette solution (also used externally) contained (in mM) 130 TMACH₃SO₃, 2 MgCl₂, 2 EGTA, 80 MES, titrated to pH 5.5 with ~20 TMAOH. In the pH 5.5 TMACl solution, TMACl replaced TMACH₃SO₃. Bath solutions at pH 7.0 had (mM) 90 TMACH₃SO₃ or TMACl, 3 CaCl₂, 1 EGTA, 100 BES, and 36–40 TMAOH. For experiments with Zn^{2+} , solutions contained PIPES buffer³⁷ without EGTA. Experiments were done at 20–25 °C. Currents are shown without leak correction. V_{rev} data were corrected for liquid junction potentials measured in each solution¹⁹.

31. Pei, J., Kim, B. H. & Grishin, N. V. PROMALS3D: a tool for multiple protein sequence and structure alignments. *Nucleic Acids Res.* **36**, 2295–2300 (2008).
32. Guindon, S. & Gascuel, O. A simple, fast, and accurate algorithm to estimate large phylogenies by maximum likelihood. *Syst. Biol.* **52**, 696–704 (2003).
33. Felsenstein, J. PROTPARS – Protein Sequence Parsimony Method <http://cmgm.stanford.edu/phylip/protpars.html> (1993).
34. Néron, B. *et al.* Mobyly: a new full web bioinformatics framework. *Bioinformatics* **25**, 3005–3011 (2009).
35. Chevenet, F., Brun, C., Bañuls, A. L., Jacq, B. & Christen, R. TreeDyn: towards dynamic graphics and annotations for analyses of trees. *BMC Bioinformatics* **7**, 439 (2006).
36. Letunic, I. & Bork, P. Interactive Tree Of Life (iTOL): an online tool for phylogenetic tree display and annotation. *Bioinformatics* **23**, 127–128 (2007).
37. Cherny, V. V. & DeCoursey, T. E. pH-dependent inhibition of voltage-gated H^+ currents in rat alveolar epithelial cells by Zn^{2+} and other divalent cations. *J. Gen. Physiol.* **114**, 819–838 (1999).